

# Ferromagnetism in Co-doped (La,Sr)TiO<sub>3</sub>

T Fix<sup>1</sup>, M Liberati<sup>2</sup>, H Aubriet<sup>3</sup>, S-L Sahonta<sup>1</sup>, R Bali<sup>1</sup>, C Becker<sup>3</sup>, D Ruch<sup>3</sup>, J L MacManus-Driscoll<sup>1</sup>, E Arenholz<sup>2</sup> and M G Blamire<sup>1</sup>

<sup>1</sup>Department of Materials Science, University of Cambridge, Pembroke Street, Cambridge CB2 3QZ, United Kingdom  
E-mail: T. Fix, tf255@cam.ac.uk

<sup>2</sup>Advanced Light Source, Lawrence Berkeley National Laboratory, Berkeley, California 94720, USA

<sup>3</sup>Laboratoire de Technologies Industrielles, Centre de Recherche Public Henri Tudor, 66 rue du Luxembourg, Esch/Alzette 4002, Luxembourg

## Abstract

The origin of ferromagnetism in Co-doped (La,Sr)TiO<sub>3</sub> epitaxial thin films is discussed. While the as-grown samples are not ferromagnetic at room temperature or at 10 K, ferromagnetism at room temperature appears after annealing the films in reducing conditions and disappears after annealing in oxidizing conditions. Magnetic measurements, x-ray absorption spectroscopy, x-ray photoemission spectroscopy, and transmission electron microscopy experiments indicate that within the resolution of the instruments the activation of the ferromagnetism is not due to the presence of pure Co.

## 1. Introduction

Owing to their potential for manipulating both the spin and charge degrees of freedom in the same material (spin electronics or spintronics), and because they provide an alternative route for spin injection into semiconductors [1], dilute magnetic semiconductors (DMSs) have been under intensive study over the past decade. While the DMS  $\text{Ga}_{1-x}\text{Mn}_x\text{As}$  has been proven to be an intrinsic ferromagnet [2], its Curie temperature is far below room temperature ( $<200\text{K}$ ) and therefore practical applications are limited. More recently, intensive theoretical and experimental studies have focused on oxide-based DMSs such as transition-metal doped ZnO [3],  $\text{TiO}_2$  [4],  $\text{SnO}_2$  [5],  $\text{Cu}_2\text{O}$  [6], and even undoped  $\text{HfO}_2$  [7], which were reported to show room temperature ferromagnetism. The origin of the ferromagnetism in these materials is still in dispute, because in early studies at least it was difficult to exclude the possibility of contamination with magnetic particles or the precipitation of magnetic metallic clusters [8,9]. The majority of the research on oxide DMS has focused on ZnO; here we report studies on Co-doped  $(\text{La,Sr})\text{TiO}_3$  [10], where room temperature ferromagnetism and large spin polarization are reported [11], while the host oxide is a strongly correlated metal [12]. This material is particularly interesting because it allows independent control of both the magnetic and carrier doping over a wide range as the La/Sr concentration ratio induces a variation from an insulator to a metal or semiconductor. We have performed studies by x-ray diffraction (XRD), x-ray absorption spectroscopy (XAS), x-ray magnetic circular dichroism (XMCD), x-ray photoemission spectroscopy (XPS), transport measurements, magnetometry, and transmission electron microscopy (TEM) on Co-doped  $(\text{La,Sr})\text{TiO}_3$  with different La/Sr ratios. We show that the ferromagnetism is not induced by Co metallic clusters within the detection limits of the instruments and we observe no clear correlation between the ferromagnetism and the carrier density.

## 2. Experimental

Stoichiometric mixtures of high purity (99.99%)  $\text{La}_2\text{O}_3$ ,  $\text{SrCO}_3$ ,  $\text{TiO}_2$ , and  $\text{Co}_3\text{O}_4$  powders were used to prepare  $\text{Sr}_{1-x}\text{La}_x\text{Ti}_{0.98}\text{Co}_{0.02}\text{O}_3$  targets with  $x=0, 0.2, 0.5, 0.8, 1$ , by milling, pre-sintering at  $900^\circ\text{C}$  for 6 hours, pressing and sintering at  $1300^\circ\text{C}$  for 6 hours. Films were grown by pulsed laser deposition from these targets using a KrF laser with a

248 nm wavelength, 10 Hz repetition rate, and energy of 150 mJ per pulse, giving a fluence of around  $1 \text{ J/cm}^2$  on the target at a substrate-target distance of 80 mm. The deposition temperature was  $600^\circ\text{C}$  and the atmosphere while depositing and cooling down was  $10^{-6}$  mbar of  $\text{O}_2$ . Prior to deposition the  $\text{NdGaO}_3$  (NGO) (001) substrates were annealed in vacuum at  $800^\circ\text{C}$  for two hours to give an atomically-defined surface structure, confirmed by an atomic force microscope (AFM) in tapping mode at room temperature. The thickness of each film is around 100 nm. The orientation and crystallinity of the films was determined by XRD with a four-circle Bruker D8 Advance diffractometer ( $\text{Cu -K}_\alpha$ ). Cross-sectional TEM was performed on the sample annealed in reducing conditions by preparation with mechanical polishing and argon ion mill at 4 kV. Lattice images of the film were taken on a JEOL 4000 EX with a spherical aberration coefficient of 0.9 mm and a point-to-point resolution of 0.17 nm, operating at 350 kV. Magnetic measurements were carried out from 300 K to 5 K with a superconducting quantum interference device (SQUID) with the magnetic field applied in the film plane. The samples were handled with extreme care to avoid contamination by extrinsic magnetic elements. Electrical contacts were made with an Al wire-bonder, the resistivity was measured by the four-probe technique and the Hall effect in a Van der Pauw configuration. XPS measurements were performed at room temperature using an Al  $\text{K}_\alpha$  (1486.7 eV) radiation as excitation source, at 12 kV and 33.4 mA in a  $10^{-9}$  mbar vacuum. The surfaces were cleaned for 5 min in  $\text{Ar}^+$  at  $5 \cdot 10^{-5}$  mbar with an energy of 1 keV. XAS and XMCD measurements on the Co  $L_{2,3}$  and Ti  $L_{2,3}$  edges were performed at the Advanced Light Source on beamline 6.3.1. The XAS signal was detected in total electron yield (TEY, surface sensitivity), at room temperature, with a magnetic field of  $\pm 2$  kOe applied parallel to the propagation direction of the x-ray beam, the latter being applied at an angle of  $30^\circ$  to the sample surface.

### 3. Results and discussion

**Figure 1** shows  $\theta$ - $2\theta$  XRD patterns for films based on  $\text{Sr}_{1-x}\text{La}_x\text{Ti}_{0.98}\text{Co}_{0.02}\text{O}_3$  with  $x=0, 0.2, 0.5, 0.8, 1$  grown on  $\text{NdGaO}_3$  (001). The films grow epitaxially without any parasitic phase detected. Asymmetric reflection XRD indicates that the epitaxial relationship is  $[100] \text{ Co-(La,Sr)TiO}_3 (001) \parallel [110] \text{ NGO (001)}$ , where  $\text{Co-(La,Sr)TiO}_3$  and NGO are

indexed in the pseudo-cubic and orthorhombic phase, respectively. The rocking curves on the Co-(La,Sr)TiO<sub>3</sub> (002) reflection give a full width at half maximum of around 0.1° which indicates a high degree of crystallite orientation. The evolution of the out-of-plane lattice parameter of the films extracted from the spectra shows a clear increase from x=0 to x=0.8, indicating the effective substitution of Sr by La. However for x=1, the lattice parameter value is lower than expected due to strain relaxation (as observed with reciprocal space maps, not shown here).

We have investigated the magnetic properties of the as-grown films at both room temperature and 10 K. No evidence of ferromagnetism or anomalous Hall effect could be evidenced within the detection limit of the instruments for any of the La,Sr ratios. In a previous work [11] it has been shown that the magnetization of the films increases when the deposition oxygen pressure decreases, suggesting role of oxygen vacancies on magnetism. Here we focus on the evolution of the ferromagnetism with successive thermal annealing at 500 °C for one hour in reducing (2% H<sub>2</sub>/Ar) or oxidizing conditions (air) (**figure 2a**). We observe that after thermal annealing under reducing conditions the films become ferromagnetic at room temperature, and then non ferromagnetic after subsequent annealing under oxidizing conditions. This evolution repeats for several cycles, after which the effect tends to vanish, indicating that the phenomenon is not fully reversible. It should be noted that no activation of ferromagnetism was observed for the clean reference NGO substrates annealed under the same conditions, which excludes any contamination by impurities from the furnace or from the substrates. Furthermore the total magnetization measured increases proportionally to the film thickness. A similar reversible activation of ferromagnetism has been observed in Co-doped ZnO, using alternating Zn interstitial incorporation and oxidation with O<sub>2</sub> [13,14]. However in our case the activation or disappearance of ferromagnetism is supposedly only linked to an oxygen-related effect as will be discussed below.

The maximum magnetization observed is about 3-4 μ<sub>B</sub>/Co, which is significantly higher than the value of pure cobalt metal (1.72 μ<sub>B</sub>/Co). This has been observed in other studies as well [10,11]. It might originate from the presence of high-and low-spin Co<sup>2+</sup> and Co<sup>3+</sup> [15], the effective moment of high spin Co<sup>3+</sup> (Co<sup>2+</sup>) being 4.90 μ<sub>B</sub> (3.87 μ<sub>B</sub>). However it

could also originate from a transferred moment on Ti or from a very small magnetic moment on a large fraction of oxygen atoms, accounting for an important overall moment, a theory which is still in debate. **Figure 2b** shows that the Curie temperature of the samples is around 460 K as reported in previous studies [10]. The samples present a significant coercivity (**figure 2c**) and uniaxial in-plane anisotropy, with the easy axis in the [010] direction of the NGO substrate (**figure 2d**). This uniaxial anisotropy can be caused when the films are fully strained and an in-plane distortion of the lattice parameters is induced by the orthorhombic NGO substrate ( $a=0.5433$  nm,  $b= 0.5503$  nm,  $c=0.7715$  nm). Most importantly, the anisotropy observed is an indication that the ferromagnetism is linked to the matrix through lattice strain and – as we will confirm with other experiments – not due to randomly dispersed inclusions that would be caused by external contamination.

We now focus on the transport properties of the samples. In a previous work where SrTiO<sub>3</sub> (STO) substrates were used to grow Co-doped (La,Sr)TiO<sub>3</sub> [16], high electronic mobilities up to  $10^4$  cm<sup>2</sup>/V s at 2 K were observed when the oxygen pressure during the growth was low. It was suggested that the high mobility may come from the STO substrate and not the thin film. We have observed indeed that after thermal annealing under vacuum or low O<sub>2</sub> pressures the STO substrates became conductive, due to the creation of oxygen vacancies. However NGO substrates remain insulating under the same conditions and are therefore suitable for transport measurements of the films. Consequently, we have measured and calculated the carrier density and mobility as a function of the temperature for a thin film based on NdGaO<sub>3</sub> (001) // La<sub>0.5</sub>Sr<sub>0.5</sub>Ti<sub>0.98</sub>Co<sub>0.02</sub>O<sub>3</sub>. **Figure 3a** shows the evolution of the mobility as a function of the temperature for a La<sub>0.5</sub>Sr<sub>0.5</sub>Ti<sub>0.98</sub>Co<sub>0.02</sub>O<sub>3</sub> sample as grown and annealed in reducing conditions. At 10 K the carrier density and mobility are respectively  $8 \cdot 10^{21}$  cm<sup>-3</sup>, 9 cm<sup>2</sup>/Vs for the as grown film and  $6 \cdot 10^{21}$  cm<sup>-3</sup>, 6 cm<sup>2</sup>/Vs for the annealed one. The mobility value is especially very far from the  $10^4$  cm<sup>2</sup>/Vs range observed in the previous work using STO substrates [16], suggesting that it was rather due to the oxygen-deficiency in the STO substrate, which is still a topical issue in the case of interfacial effects [17]. The values obtained here are quite close to previous measurements on La<sub>0.5</sub>Sr<sub>0.5</sub>TiO<sub>3</sub> or La<sub>0.67</sub>Sr<sub>0.33</sub>Ti<sub>0.98</sub>Co<sub>0.02</sub>O<sub>3</sub> films grown on other substrates [16,18]. The

carriers are electrons and the value for the carrier concentration is in good agreement with around 0.5 carrier per formula unit as expected from the film composition [11]. There is no large change in carrier concentration arising from the annealing under reducing conditions, which means that the introduction of oxygen vacancies induces a small variation in electron concentration. In fact, the mobility and carrier density are slightly reduced after the annealing, implying defect trapping and scattering. While the La,Sr ratio induces strong changes in the carrier density and mobility (**Table I**), it does not cause any consistent variation of the magnetic moment. This could be interpreted as a sign that the ferromagnetism in this system is rather activated by defects than mediated by carriers, however there is a need for further and novel characterizations of defects and oxygen vacancies in DMSs to support or infer such hypotheses.

Anomalous Hall effect was observed at 10 K on a  $\text{Sr}_{0.5}\text{La}_{0.5}\text{Ti}_{0.98}\text{Co}_{0.02}\text{O}_3$  sample annealed in reducing conditions, as shown in **figure 3b**. It is commonly assumed that the observation of anomalous Hall effect is a good indicator of intrinsic ferromagnetism [19]. However, there seems to be a contradiction as superparamagnetism and anomalous Hall effect have been simultaneously observed in  $\text{Co}:\text{TiO}_2$  [20] and Co-doped  $(\text{La,Sr})\text{TiO}_3$  [21]. Therefore it is necessary to investigate if there is pure Co in our system that could be superparamagnetic.

After having investigated the conditions for the appearance of ferromagnetism, we now try to understand its origin: is it intrinsic or extrinsic? The quality of the epitaxy is confirmed by high resolution TEM as shown in **figure 4a**, and no Co clusters or secondary phases can be observed within the detection limits of the instrument. This is consistent with the electron diffraction pattern in **figure 4b** which shows only diffraction periodicities relating to the  $(\text{La,Sr})\text{TiO}_3$  crystalline phase. To confirm the presence or absence of Co clusters, thin films composed of  $\text{La}_{0.5}\text{Sr}_{0.5}\text{Ti}_{0.98}\text{Co}_{0.02}\text{O}_3$  have been analyzed by XPS at room temperature. **Figure 5** shows a scan with the Co contribution for an as-grown sample and for the same sample after annealing in reducing conditions. According to previous work [22], the  $\text{Co}^0$  and  $\text{Co}^{2+}$  ( $\text{Co}^{3+}$ ) contributions should be shifted in energy by only about 2.8 eV (0.9 eV respectively). Therefore, the absolute binding energies do not always allow the determination of the Co chemical environment. Here for

the as-grown film Co  $2P_{3/2}$  and  $2P_{1/2}$  contributions are observed at 779.7 and 795.5 eV respectively. The presence of high intensity satellite peaks at 784.8 and 801.5 eV (marked *s* in the figure) indicates the formation of octahedrally coordinated  $\text{Co}^{2+}$  [23,24]. No significant change in the spectra was observed after the annealing.

XAS and XMCD measurements were performed at the Co  $L_{2,3}$  and Ti  $L_{2,3}$  edges of  $\text{La}_{0.5}\text{Sr}_{0.5}\text{Ti}_{0.98}\text{Co}_{0.02}\text{O}_3$  thin films. **Figure 6** shows x-ray absorption spectra at room temperature at the Co  $L_{2,3}$  and Ti  $L_{2,3}$  edges for an as-grown sample and a sample annealed in reducing conditions. No XMCD signal could be measured in total electron yield for Co  $L_{2,3}$  and Ti  $L_{2,3}$  edges, indicating that these states are not polarized. The Co  $L_{2,3}$  XAS spectra shows a multiplet structure typical of  $\text{Co}^{2+}$ , both for the as-grown and annealed samples, which is in agreement with the XPS experiment. This proves clearly that the ferromagnetism does not originate from metallic Co. However, further experiments will be needed to investigate if the ferromagnetism originates from oxygen deficiencies, as suggested in similar XMCD studies [25,26].

#### 4. Conclusions

We have observed the activation and deactivation of ferromagnetism in Co-doped (La,Sr)TiO<sub>3</sub> epitaxial thin films. Magnetic measurements, XPS, XAS and TEM indicate that the activation of the ferromagnetism is not due to the presence of pure Co, in  $\text{La}_{0.5}\text{Sr}_{0.5}\text{Ti}_{0.98}\text{Co}_{0.02}\text{O}_3$  samples, and it is not carrier mediated. Therefore this system is very promising and further experiments and theoretical calculations will be necessary to investigate the role of the oxygen.

#### Acknowledgments

The Advanced Light Source is supported by the Director, Office of Science, Office of Basic Energy Sciences, of the U.S. Department of Energy under Contract No. DE-AC02-05CH11231. We acknowledge the financial support from the European Union under Framework 6 program for the Nanoxide project (Novel Nanoscale Devices based on functional Oxide Interfaces). We are grateful to Mary Vickers for fruitful discussions on XRD.

- [1] Wolf S A, Awschalom D D, Buhrman R A, Daughton J M, von Molnár S, Roukes M L, Chtchelkanova A Y, Treger D M 2001 Spintronics: A spin-based electronics vision for the future *Science* **294**, 1488
- [2] Ohno H, Shen A, Matsukura F, Oiwa A, Endo A, Katsumoto S, and Iye Y 1996 (Ga,Mn)As: A new diluted magnetic semiconductor based on GaAs *Appl. Phys. Lett.* **69**, 363
- [3] Ueda K, Tabata H, Kawai T 2001 Magnetic and electric properties of transition-metal-doped ZnO films *Appl. Phys. Lett.* **79**, 988
- [4] Matsumoto Y, Murakami M, Shono T, Hasegawa T, Fukumura T, Kawasaki M, Ahmet P, Chikyow T, Koshihara S, Koinuma H 2001 Room-temperature ferromagnetism in transparent transition metal-doped titanium dioxide *Science* **291**, 854
- [5] Ogale S B, Choudhary R J, Buban J P, Lofland S E, Shinde S R, Kale S N, Kulkarni V N, Higgins J, Lanci C, Simpson J R, Browning N D, Das Sarma S, Drew H D, Greene R L, Venkatesan T 2003 High temperature ferromagnetism with a giant magnetic moment in transparent Co-doped  $\text{SnO}_{2-\text{delta}}$  *Phys. Rev. Lett.* **91**, 077205
- [6] Liu Y L, Harrington S, Yates K A, Wei M, Blamire M G, MacManus-Driscoll J L, Liu Y C 2005 Epitaxial, ferromagnetic  $\text{Cu}_{2-x}\text{Mn}_x\text{O}$  films on (001) Si by near-room-temperature electrodeposition *Appl. Phys. Lett.* **87**, 222108
- [7] Venkatesan M, Fitzgerald C B, and Coey J M D 2004 Unexpected magnetism in a dielectric oxide *Nature (London)* **430**, 630
- [8] Belghazi Y, Schmerber G, Colis S, Rehspringer J L, and Dinia A 2006 Extrinsic origin of ferromagnetism in ZnO and  $\text{Zn}_{0.9}\text{Co}_{0.1}\text{O}$  magnetic semiconductor films

prepared by sol-gel technique *Appl. Phys. Lett.* **89**, 122504

[9] Park J H, Kim M G, Jang H M, Ryu S, Kim Y M 2004 Co-metal clustering as the origin of ferromagnetism in Co-doped ZnO thin films *Appl. Phys. Lett.* **84**, 1338

[10] Zhao Y G, Shinde S R, Ogale S B, Higgins J, Choudhary R J, Kulkarni V N, Greene R L, Venkatesan T, Lofland S E, Lanci C, Buban J P, Browning N D, Das Sarma S, Millis A J 2003 Co-doped  $\text{La}_{0.5}\text{Sr}_{0.5}\text{TiO}_{3-\text{delta}}$ : Diluted magnetic oxide system with high Curie temperature *Appl. Phys. Lett.* **83**, 2199

[11] Herranz G, Ranchal R, Bibes M, Jaffrès H, Jacquet E, Maurice J-L, Bouzheouane K, Wyczisk F, Tafra E, Basletic M, Hamzic A, Colliex C, Contour J-P, Barthélémy A, and Fert A 2006 Co-doped  $(\text{La,Sr})\text{TiO}_{(3-\text{delta})}$  : a high Curie temperature diluted magnetic system with large spin polarization *Phys. Rev. Lett.* **96**, 027207

[12] Tokura Y, Taguchi Y, Okada Y, Fujishima Y, Arima T, Kumagai K, Iye Y 1993 Filling dependence of electronic properties on the verge of metal–Mott-insulator transition in  $\text{Sr}_{1-x}\text{La}_x\text{TiO}_3$  *Phys. Rev. Lett.* **70**, 2126

[13] Schwartz D A and Gamelin D R 2004 Reversible 300 K ferromagnetic ordering in a diluted magnetic semiconductor *Adv. Mater.* **16**, 2117

[14] Khare N, Kappers M J, Wei M, Blamire M G, MacManus-Driscoll J L 2006 Defect-induced ferromagnetism in Co-doped ZnO *Adv. Mater.* **18**, 1449

[15] Moritomo Y, Higashi K, Matsuda K, and Nakamura A 1997 Spin-state transition in layered perovskite cobalt oxides:  $\text{La}_{2-x}\text{Sr}_x\text{CoO}_4$  ( $0.4 < x < 1.0$ ) *Phys. Rev. B* **55**, R14725

[16] Herranz G, Basletic M, Bibes M, Ranchal R, Hamzic A, Tafra E, Bouzheouane K, Jacquet E, Contour J P, Barthélémy A and Fert A 2006 Full oxide heterostructure combining a high-T-C diluted ferromagnet with a high-mobility conductor *Phys. Rev.*

*B* **73**, 064403

- [17] Fix T, MacManus-Driscoll J L, Blamire M G 2009 Delta-doped LaAlO<sub>3</sub>/SrTiO<sub>3</sub> interfaces *Appl. Phys. Lett.* in press.
- [18] Vilquin B, Kanki T, Yanagida T, Tanaka H, Kawai T 2005 Effect of Sr doping on LaTiO<sub>3</sub> thin films *Appl. Surf. Sci.* **244**, 494
- [19] Wang Z, Wang W, Tang J, Tung L D, Spinu L, and Zhou W 2003 Extraordinary Hall effect and ferromagnetism in Fe-doped reduced rutile *Appl. Phys. Lett.* **83**, 518
- [20] Shinde S R, Ogale S B, Higgins J S, Zeng H, Millis A J, Kulkarni V N, Ramesh R, Greene R L, and Venkatesan T 2004 Co-occurrence of Superparamagnetism and anomalous Hall effect in highly reduced cobalt-doped rutile TiO<sub>2-delta</sub> films *Phys. Rev. Lett.* **92**, 166601
- [21] Zhang S X, Yu W, Ogale S B, Shinde S R, Kundaliya D C, Tse W-K, Young S Y, Higgins J S, Salamanca-Riba L G, Herrera M, Fu L F, Browning N D, Greene R L, and Venkatesan T 2007 Magnetism and anomalous hall effect in Co-(La,Sr)TiO<sub>3</sub> *Phys. Rev. B* **76**, 085323
- [22] Ikonov J, Stoychev D, Marinova Ts 2000 XPS and SEM characterization of electrodeposited transition metals on zirconia *Appl. Surf. Sci.* **161**, 94
- [23] Petitto S C, Marsh E M, Carson G A, Langell M A 2008 Cobalt oxide surface chemistry: The interaction of CoO(100), Co<sub>3</sub>O<sub>4</sub>(110) and Co<sub>3</sub>O<sub>4</sub>(111) with oxygen and water *J. Mol. Catal.* **281**, 49
- [24] Kim J-G, Pugmire D L, Battaglia D, Langell M A 2000 Analysis of the NiCo<sub>2</sub>O<sub>4</sub> spinel surface with Auger and X-ray photoelectron spectroscopy *Appl. Surf. Sci.* **165**, 70
- [25] Tietze T, Gacic M, Schütz G, Jakob G, Brück S, and Goering E 2008 XMCD studies on Co and Li doped ZnO magnetic semiconductors *New J. Phys.* **10**, 055009
- [26] Barla A, Schmerber G, Beaupaire E, Dinia A, Bieber H, Colis S, Scheurer F,

Kappler J-P, Imperia P, Nolting F, Wilhelm F, Rogalev A, Müller D, and Grob J J 2007  
Paramagnetism of the Co sublattice in ferromagnetic  $Zn_{1-x}Co_xO$  films *Phys. Rev. B* **76**,  
125201

**Figure 1.** XRD  $\theta$ - $2\theta$  spectrum of  $\text{NdGaO}_3$  (001) //  $\text{Sr}_{1-x}\text{La}_x\text{Ti}_{0.98}\text{Co}_{0.02}\text{O}_3$  (100 nm) for  $x=0, 0.2, 0.5, 0.8, 1$ .

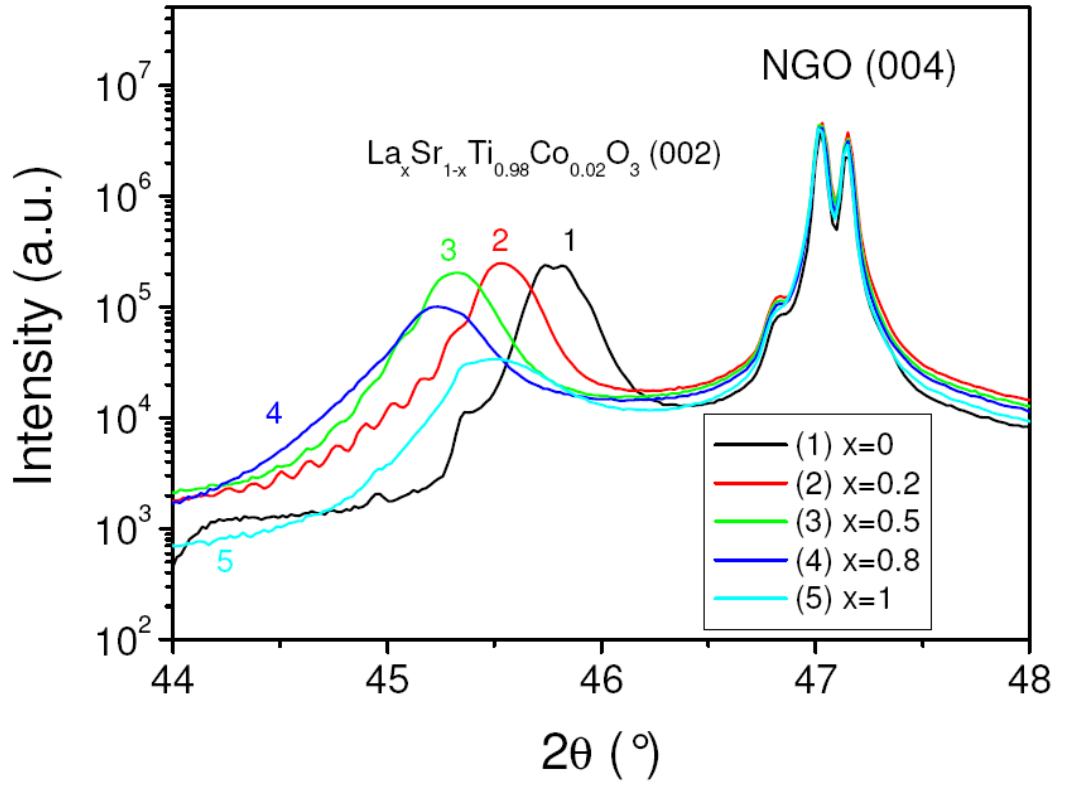


**Figure 2.** a) Evolution of the magnetization at room temperature for a  $\text{LaTi}_{0.98}\text{Co}_{0.02}\text{O}_3$  sample after successive annealing in reducing or oxidizing conditions. Similar results are obtained for different La/Sr concentration ratios. For a  $\text{La}_{0.5}\text{Sr}_{0.5}\text{Ti}_{0.98}\text{Co}_{0.02}\text{O}_3$  sample annealed in reducing conditions: b) Evolution of the saturation magnetization as a function of the temperature c) Magnetization curve at room temperature d) Coercive field as a function of the in-plane orientation. Zero angle is along NGO [100].

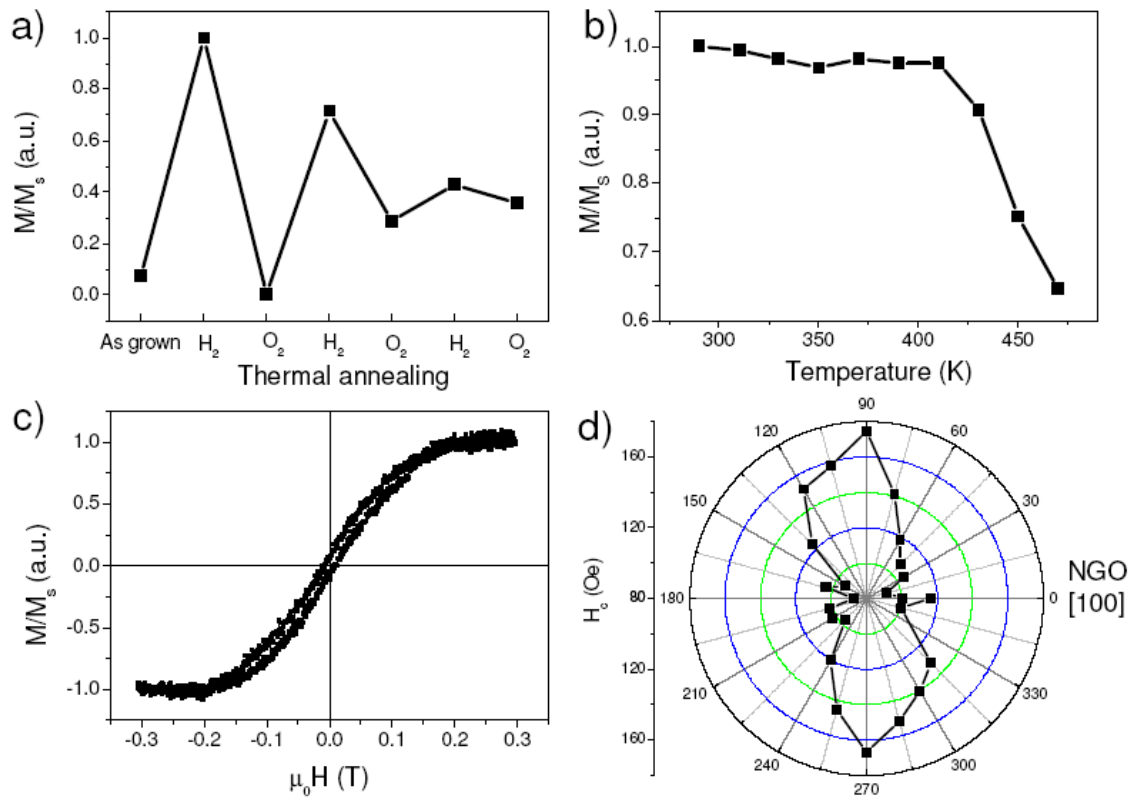


**Figure 3.** a) Mobility as a function of the temperature for  $\text{Sr}_{0.5}\text{La}_{0.5}\text{Ti}_{0.98}\text{Co}_{0.02}\text{O}_3$  as grown and annealed in reducing conditions. b) Anomalous Hall effect measured at 10 K on a  $\text{Sr}_{0.5}\text{La}_{0.5}\text{Ti}_{0.98}\text{Co}_{0.02}\text{O}_3$  annealed in reducing conditions. The ordinary Hall effect has been subtracted for viewing purposes, the field has been varied from 9 T to -9 T and then back to 9 T.

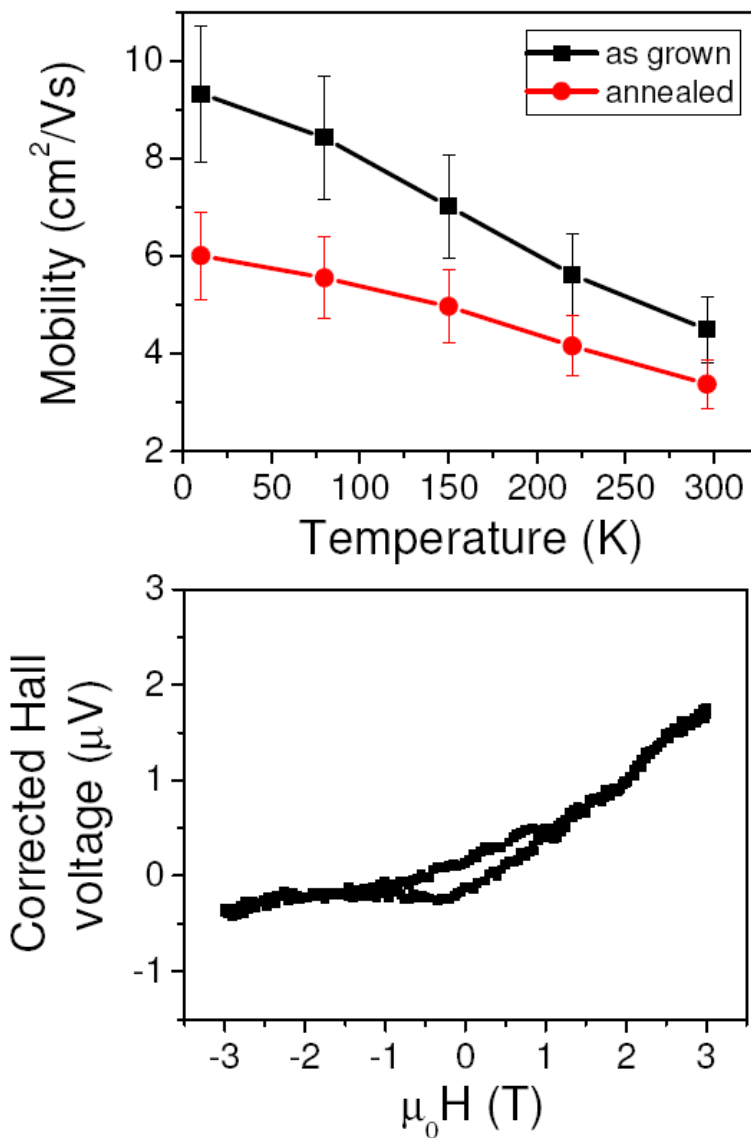


**Figure 4.** a) High resolution TEM image, b) diffraction pattern along NGO [100] of a  $\text{La}_{0.5}\text{Sr}_{0.5}\text{Ti}_{0.98}\text{Co}_{0.02}\text{O}_3$  film annealed in reducing conditions.

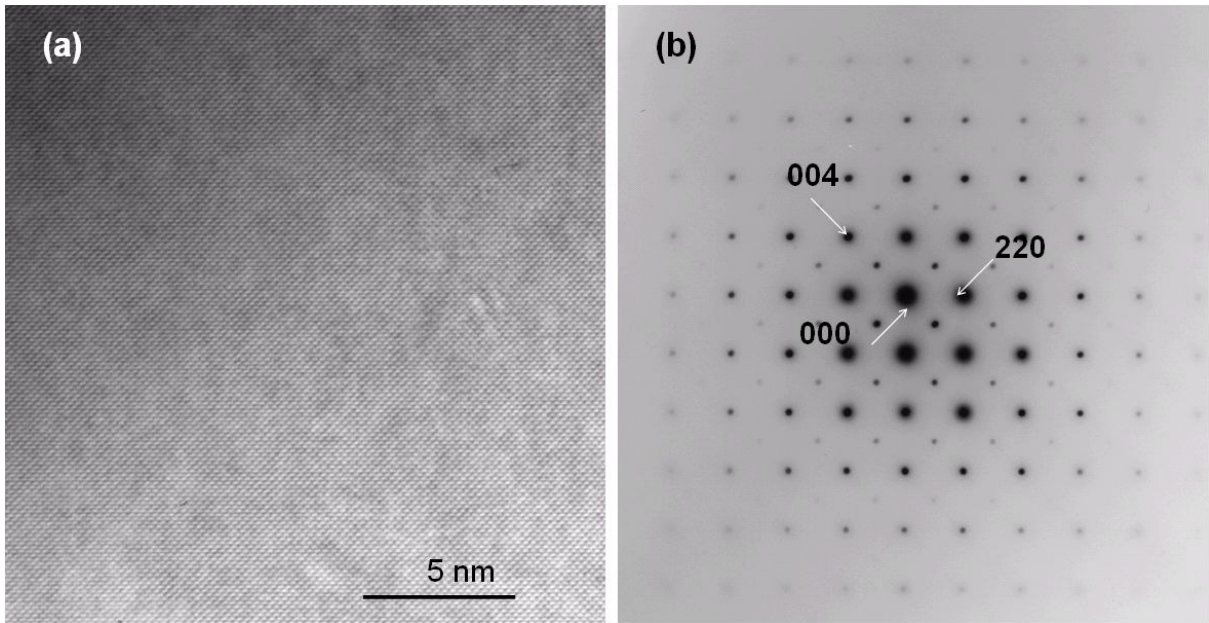


**Figure 5.** XPS spectra showing Co<sup>2+</sup> contribution for La<sub>0.5</sub>Sr<sub>0.5</sub>Ti<sub>0.98</sub>Co<sub>0.02</sub>O<sub>3</sub> as grown and annealed in reducing conditions.

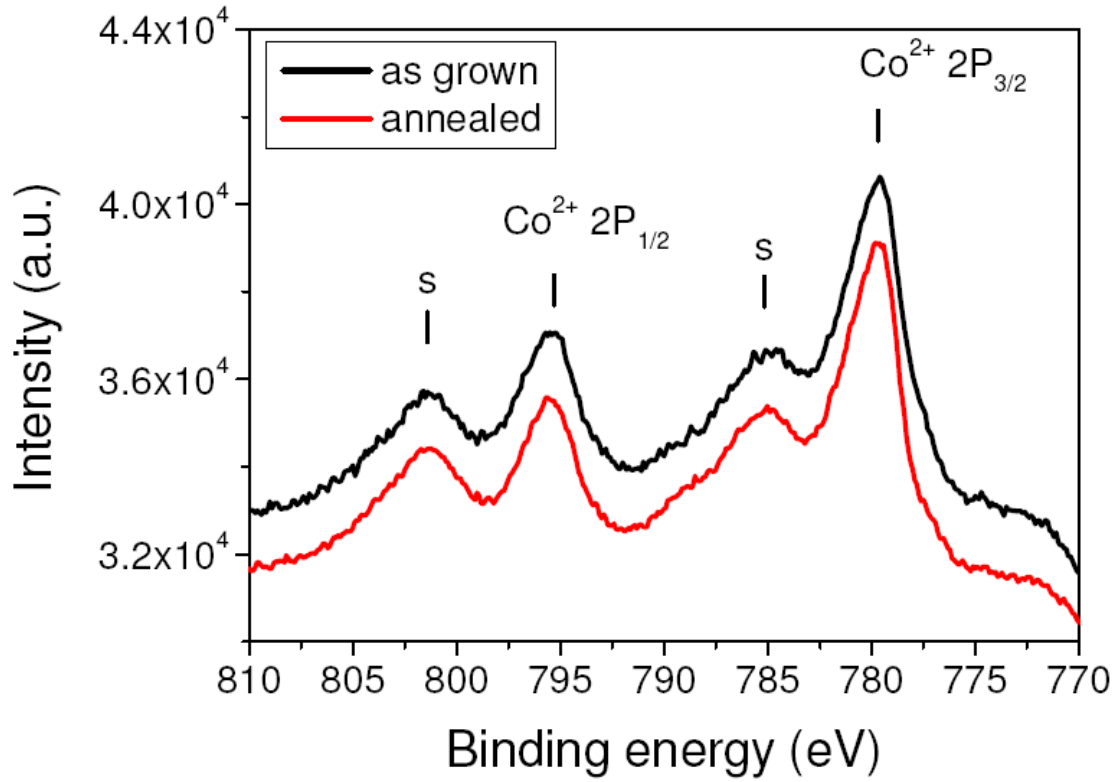


**Figure 6.** XAS spectra at 300 K at Co and Ti  $L_{2,3}$  edges for  $\text{La}_{0.5}\text{Sr}_{0.5}\text{Ti}_{0.98}\text{Co}_{0.02}\text{O}_3$  as grown and annealed in reducing conditions.

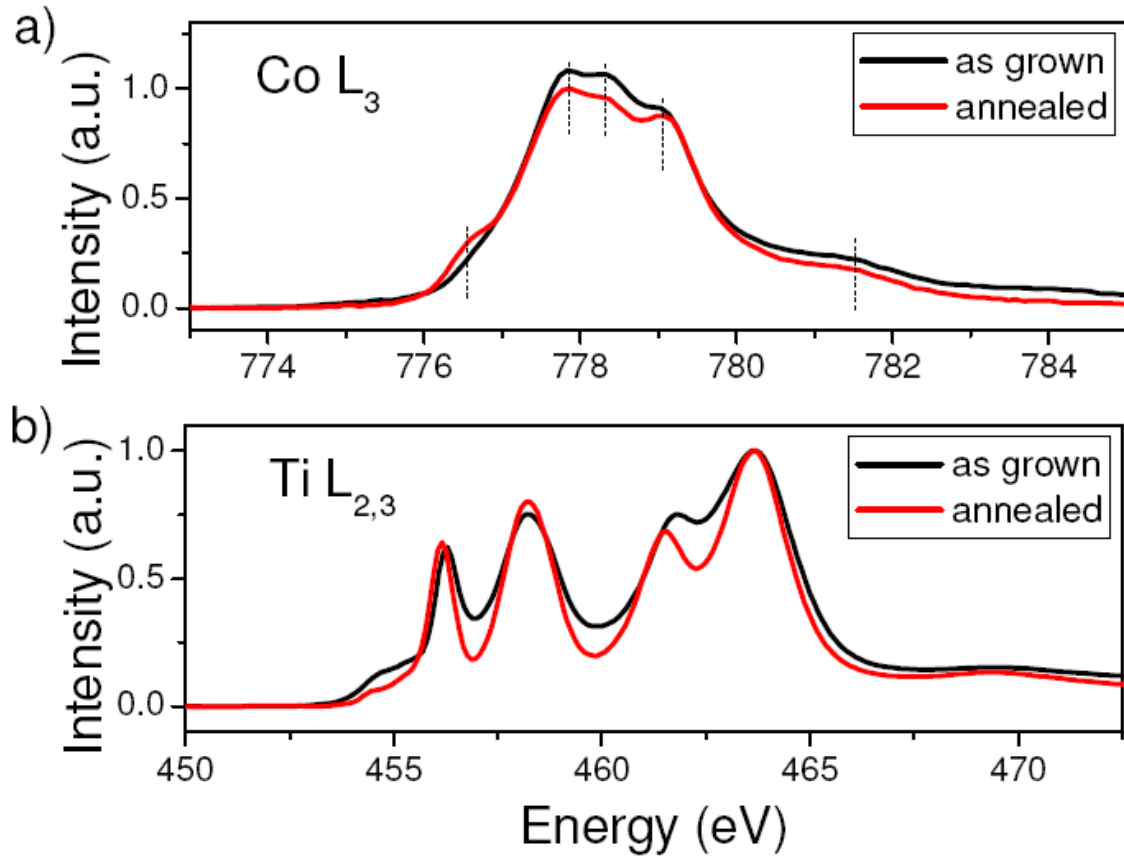


**Table I: evolution of the carrier density and mobility at 220 K in  $\text{Sr}_{1-x}\text{La}_x\text{Ti}_{0.98}\text{Co}_{0.02}\text{O}_3$  thin films.**

x	Carrier density ( $10^{21} \text{ cm}^{-3}$ )	Mobility ( $\text{cm}^2/\text{Vs}$ )
0	insulating	
0.2	2.4	5.2
0.5	6.0	4.2
0.8	9.9	0.65
1	0.082	0.021